Quaternary Research 73 (2010) 374–384

Contents lists available at ScienceDirect

Quaternary Research

journal homepage: www.elsevier.com/locate/yqres

New insights on Illinoian deglaciation from deposits of Glacial Lake Quincy, central Indiana

J.R. Wood, S.L. Forman *, J. Pierson, J. Gomez

Department of Earth and Environmental Sciences, 845 W. Taylor Street, University of Illinois at Chicago, Chicago, IL 60607, USA

ARTICLE INFO

Article history:
Received 16 March 2009
Available online 30 December 2009

Keywords:
Illinoian limit
Glacial lacustrine sediments
Optical dating

ABSTRACT

The deposits of Glacial Lake Quincy overlie a diamicton associated with the classically defined Illinoian limit in central Indiana. This lake covered at least 180 km^2 with a depth of >20 m and developed when the Illinoian ice sheet retreated 15 km from the maximum limit, causing lake impoundment against Devore Ridge. Overflow from Glacial Lake Quincy eroded across the ridge forming a number of steeped-walled outlets. A section along Mill Creek exposes a sedimentologic sequence associated with Glacial Lake Quincy from a subglacial diamicton to ice-proximal to ice-distal glacial lacustrine sediments. We report new optical ages by multiple aliquot regenerative dose procedure for the fine-grained rhythmically bedded sediments presumed to represent the lowest energy depositional facies, dominated by suspension settling, which maximized sunlight exposure. In turn, optical ages were determined on the fine-grained (4–11 μm) polymineral and quartz fractions under infrared and blue excitation, which yielded statistically similar ages. Optical ages span from ca. 170 to 108 ka, with the average of 16 optical ages indicating deglaciation at ca. 135 ka, generally coincident with Marine Oxygen Isotope Stage 6-to-5 transition and rise in global sea level.

Introduction

A classic glacial geologic concept is the Illinoian limit in mid-continental North America (Fig. 1, inset). This limit may incorporate glacial limits of various ages, which are by definition, older than the last glacial maximum (e.g., Leverett, 1898; Frye et al., 1965; Flint, 1971, 550–555; Johnson, 1986; Jennings et al., 2007). Early field observations distinguished Illinoian terrain from younger Wisconsinan glaciated areas by the position of inferred end moraines, depth of leaching of carbonate minerals, identification of buried soils, and the extent of fluvial dissection (e.g., Leverett, 1898; Malott, 1926; Thornbury, 1936; Frye, 1968). Later studies defined Illinoian drift based on the extent of soil development (cf. Ruhe, 1969) and stratigraphic relation between glaciogenic sediments and buried soils (cf. Frye et al., 1965; Willman and Frye, 1970; Follmer, 1983, 1996; Stiff and Hansel, 2004).

The diagnostic deposit of the Illinoian glaciation is the Glasford Formation in central Illinois, which is composed of glacial diamictons and outwash and often buries the Yarmouth Geosol (Willman and Frye, 1970, 52–54). The Sangamon Geosol is developed in the Glasford Formation and other glaciogenic correlative units like the Loveland Loess (Willman and Frye, 1970, 54). Chronologic control of the Illinoian glaciations is defined principally by luminescence dating of the Loveland Loess. The Loveland Loess at its type locality in western Iowa yielded thermoluminescence and infrared stimulated luminescence ages of ca. 125–160 and 146–165 ka, respectively, and is correlative generally with glacial conditions during Marine Oxygen Isotope Stage (MIS) 6 (Forman and Pierson, 2002). Loveland Loess in other localities within the Missouri and Mississippi river basins yielded luminescence ages of ca. 130–185 ka (Maat and Johnson, 1996; Rodbell et al., 1997; Markewich et al., 1998; Forman and Pierson, 2002) and similar to ^{10}Be inventory ages (Curry and Pavich 1996; Markewich et al., 1998). Quartz grains from glacial fluvial sands within the ancient Mississippi Valley in north-central Illinois and beneath an Illinoian till yielded optical ages of ca. 160 ka (McKay and Berg, 2008).

A number of studies of loess and other sedimentary successions in Illinois conclude that there is lack of evidence for glaciations between MIS 5 and 3 (Curry, 1989; Curry and Pavich 1996; Grimley, 2000). However, there are also numerous localities, presumed to be correlative to the Loveland Loess type locality, that yield younger luminescence ages ca. 60-100 ka (Rodbell et al., 1997; Forman and Pierson, 2002). A recent core from southern Illinois confirms the presence of two inter-Sangamonian loesses and an early Roxana silt member (Markham) underscoring the possibility of the expansion of the Laurentide ice sheet into the Mississippi River catchment numerous times between ca. 130 and 50 ka (Wang et al., 2009), consistent with meltwater records from the Gulf of Mexico (Joyce et al., 1993; Tripsanas et al., 2007).

This study documents proglacial lake sediments and optical ages for a small portion of the Illinoian limit in Mill Creek Valley, central Indiana (Fig. 1). The Illinoian limit has broad spatial continuity in the

* Corresponding author.
E-mail address: slf@uic.edu (S.L. Forman).

0033-5894/$ – see front matter © 2009 University of Washington. Published by Elsevier Inc. All rights reserved.
doi:10.1016/j.yqres.2009.10.008

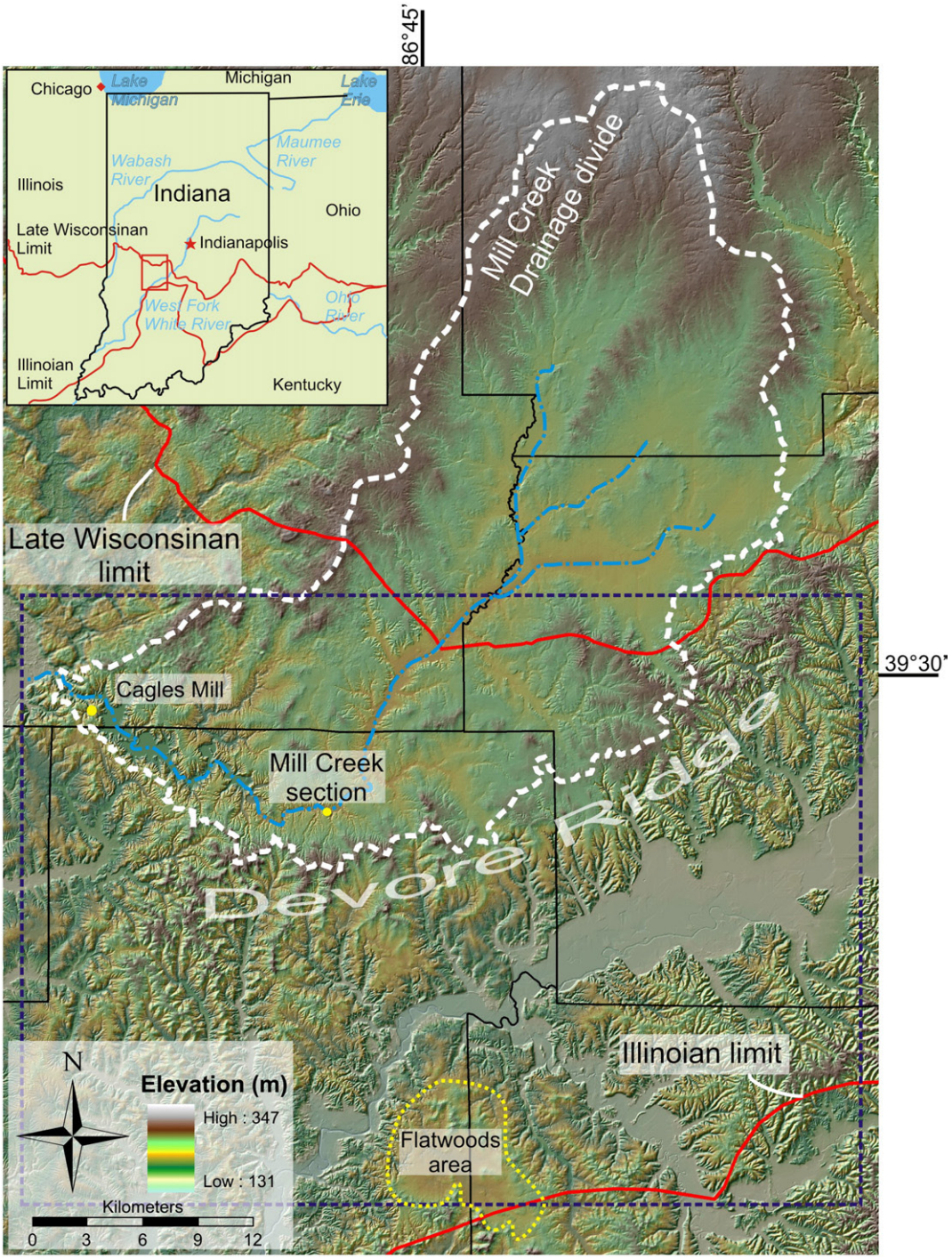

Figure 1. The Mill Creek Valley of central Indiana located between the Late Wisconsinan and Illinoian glacial limits. Devore Ridge is the southern limit of the valley and contains deeply incised and underfit stream valleys that channeled water from Glacial Lake Quincy. Glacial lacustrine sediments in the Mill Creek Valley and glacial geomorphic features on Devore Ridge provide insights to the extent of the lake and indirectly the timing the ice margin position. The Flatwoods area (Malott, 1922; Jacobs, 1994) is a flat, elevated plain also attributed to a proglacial lake of Illinoian age. Blue inscribed line is location of Figure 2.

Midwest with the Vandalia Till Member of the Glasford Formation, a recognized Illinoian glacial diamicton across eastern Illinois and central Indiana (Bleuer, 1991; Hall and Anderson, 2001; Jacobs, 1994; Willman and Frye, 1970). Farther to the south, at the farthest extent of glaciation in southern Indiana, is evidence for formation of another proglacial lake, Flatwoods, which hosts a complex weathering profile at the surface and is correlative with the Sangamon Geosol (Jacobs, 1994).

The Illinoian and Wisconsinan glacial limits are within 15 km of each other in central Indiana. This Illinoian glacial limit is demarcated by greatest extent of glaciogenic sediments, including diamictons and waterlain silts (Malott, 1922, 210–211; Thornbury, 1936; Gray, 1988). Early studies in the Mill Creek drainage (Fig. 1) identified a large flat plain composed of stratified silts at distinct elevations and lower than adjacent moraines (Collett, 1876; Brown, 1884; Addington, 1926; Malott, 1922, 210–211). These landforms and deposits were the basis for inferring the presence of a proglacial lake, called Quincy, associated with the Illinoian limit. Glacial Lake Quincy is stratigraphically the lowest of the recognized proglacial lakes in the Mill Creek Valley with outlets eroded into the adjacent

https://doi.org/10.1016/j.yqres.2009.10.008 Published online by Cambridge University Press

interfluve, here named Devore Ridge (Addington, 1926; Malott, 1922, 210-211). Early interpretations of the age of the sediment found in wells and exposures were based on the degree of carbonate leaching (Malott, 1922, 210–211; Addington, 1926; Thornbury, 1940). The carbonate content in the lake sediments is low, presumably reflecting subarial exposure, and is similar to the glacial diamictons located to the west end of Mill Creek Valley, which are correlative to Illinoian glacial diamictons of southern Illinois (Malott, 1926; Thornbury, 1950).

Pioneering glacial geologic field mapping has inferred the presence of Glacial Lake Quincy in central Indiana that formed after deglaciation from the maximum Illinoian limit (Malott, 1926; Addington, 1926; Thornbury, 1940). This study re-identifies diamictons and proglacial lacustrine sediments associated with Glacial Lake Quincy (Thornbury, 1950; Autio, 1990). These sediments reflect proglacial lacustrine deposition upon deglaciation from the classic Illinoian limit. In turn, optical dating of far-transported laminated silts and clays, dominated by suspension settling, provides chronologic control. This assessment yields a direct metric on the extent and age of the Illinoian limit in central Indiana.

Geomorphology of the Glacial Lake Quincy basin

The size of Glacial Lake Quincy is controlled by the location of the ice sheet margin in reference to the Mill Creek drainage and Devore Ridge. It is inferred that Glacial Lake Quincy formed with an ice sheet position north of Devore Ridge and ice sheet blockage of the western part of Mill Creek (Figs. 1 and 2). The level of this lake is controlled principally through the elevation of outlets incised through Devore Ridge (Fig. 2). The full extent of Glacial Lake Quincy is unknown. A minimum estimate of lake extent, 180 km^2, is based on the distribution of lake sediments (Thornbury, 1950; Autio, 1990) relative to the inferred elevation of outlets (Fig. 2). A potential recessional glacial limit of Illinoian age (Fig. 2) that may have impounded Glacial Lake Quincy is demarcated by a moraine remnant on the western margin of the Mill Creek drainage basin (Fig. 1; Thornbury, 1940; 1950; McGrain, 1949) and which may be correlative with glacial diamictons identified in the Cagles Mill section (Wayne, 1963; Hall and Anderson, 2001) and the upper diamicton within the Flatwoods area (Fig. 1; Jacobs, 1994). We infer that an east–west trending ice margin dammed the Mill Creek

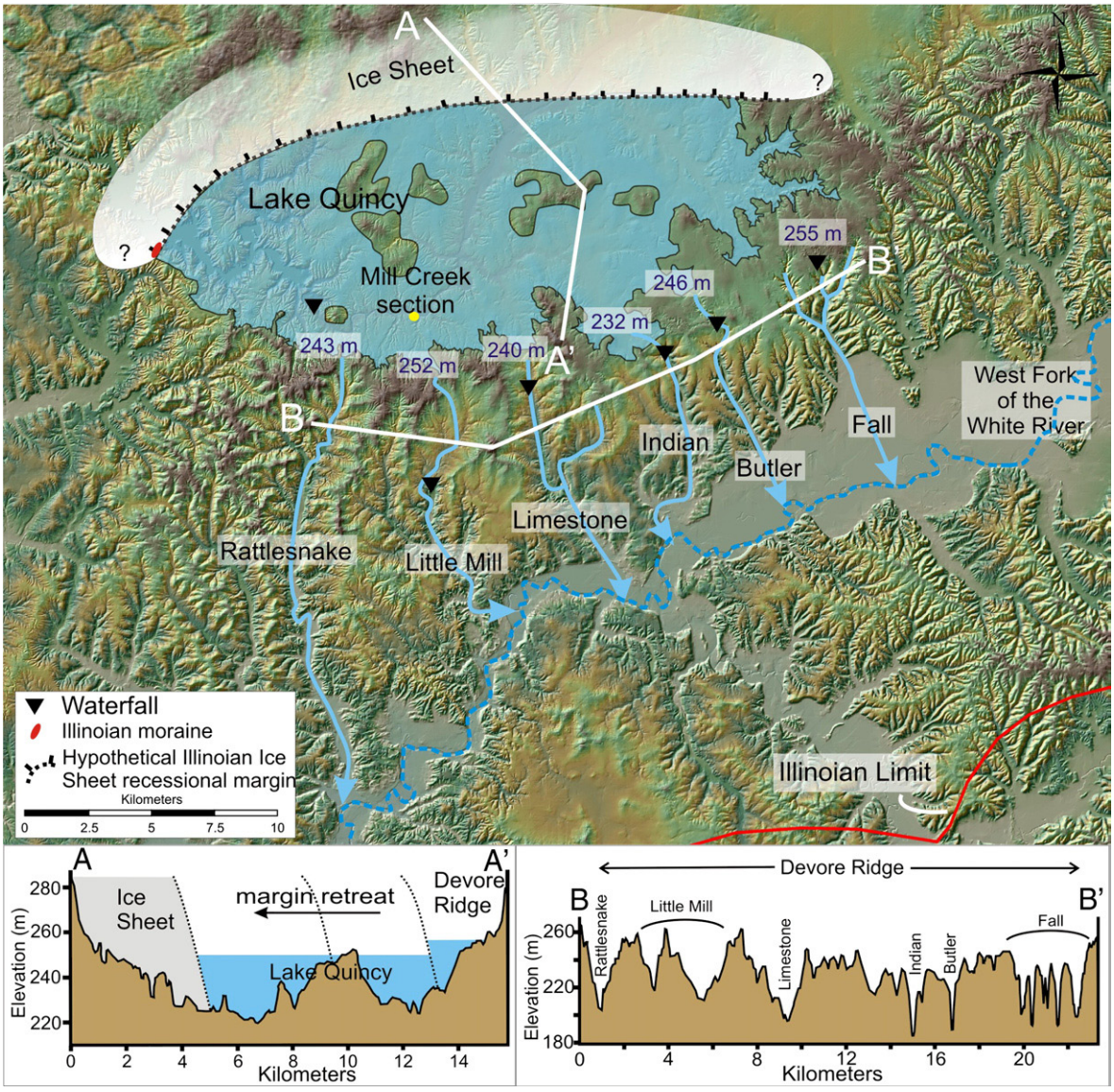

Figure 2. Minimum extent of Glacial Lake Quincy assuming all mapped glacial sediments are correlative and of Illinoian age. Lake depth is >20 m with a minimum extent of ~180 km^2. Cross section A-A' indicates hypothetical recession of the Illinoian ice margin from Devore Ridge creating Glacial Lake Quincy. Cross section B-B' shows outlets on Devore Ridge and the depth of incision.

https://doi.org/10.1016/j.yqres.2009.10.008 Published online by Cambridge University Press

Valley and this hypothetical ice margin formed somewhat parallel to the mapped Illinoian limit (Fig. 2).

Ice-margin oscillations would have controlled the routing of lake drainage and duration of an outlet across Devore Ridge. Likewise, an ice advance could close low-elevation outlets, creating high stands that drained through previously abandoned and/or elevationally higher outlets. Previous investigations by Autio (1990) show that lacustrine sediments are intercalated with diamictons and eolian silts, evidence that proglacial lakes impounded by an ice sheet repeatedly flooded the valley. The drainages incised across Devore Ridge are particularly distinctive and indicate appreciably higher discharge than current conditions. Valleys are deeply incised (20–25 m of relief) with clearly underfit streams (Fig. 2). Most valleys have mid-drainage waterfalls or steep-sided bedrock channels extending nearly to the interfluves, the result of deep incision. This incision is so deep that Devore Ridge drainages like Fall, Butler, Indian and Limestone creeks do not drain into Mill Creek but drain to the south into the White River (Fig. 2). However, Indian, Butler and Fall Creek outlets were probably reoccupied with formation of proglacial lakes after ca. 50 ka (cf. Autio, 1990; Wood et al., 2007), rejuvenating valley incision.

The highest inferred outlet associated with Glacial Lake Quincy is at 252 m elevation and is located at the interfluve of Mill Creek and Little Mill Creek (Fig. 2). There are several other inferred outlets between 243 and 230 m elevation incised into Devore Ridge (Fig. 2), and relative to the elevation of Mill Creek this suggests a lake depth of >20 m for Glacial Lake Quincy.

Optical dating

Sediments targeted for optical dating are horizontally laminated clayey silts to silty clays, reflecting ice-distal sedimentation, dominated by suspension settling. This sedimentary facies was chosen purposely for optical dating because of the extended light exposure with transport. Sediments are inferred to be transported kilometers in the upper few meters of the proglacial lake and, with turbulent transport, repeatedly exposed to filtered sunlight. A recent study shows a ~99% reduction in luminescence after 24 h of light exposure of quartz and feldspar transported in 1-m layer with moderate turbidity, despite wavelength attenuation below 500 nm and above 750 nm (Sanderson et al., 2007). Rendell et al. (1994) demonstrated that quartz was solar reset after 3 h beneath >10 m of calm water. Our laboratory experiments confirm this sensitivity to solar resetting (cf. Godfrey-Smith et al., 1988) for the fine silt fraction that shows >90% reduction in the polymineral and quartz luminescence within the first 1 to 2 min of sunlight exposure. These luminescence components have varying photo sensitivities (Godfrey-Smith et al., 1988) but have uniform and low solar reset level (indicated by similarity in age; Table 1), which are significant to resolve a depositional age (cf. Wintle, 1997).

Multiple-aliquot regeneration (MAR) procedures with component dose normalization (Jain et al., 2003) were used in this study to estimate the equivalent dose on fine-grained polymineral and quartz fraction from sediments (Fig. 3; Table 1). Initially, fine grains (4–11 μm) were extracted by suspension settling follow Stokes Law after organics and carbonate was removed with soaking in H_2O_2 and in HCl, respectively (cf. Aitken 1985, 227–228). Quartz extracts on the fine-grained fraction were isolated subsequently by digestion in hydrofluosilicic acid (silica saturated) for 6 days (Berger et al., 1980; Roberts, 2007). Solar resetting of aliquots prior to MAR analysis was accomplished by 8-h illumination from a 275W General Electric Mercury Vapor Sunlamp, removing any pre-existing electrons within accessible photosensitive traps while inducing minimal dose sensitivity changes (Richardson, 1994). To track dose-based sensitivity changes, an initial laboratory normalization dose of ~82 Gy β was given to each aliquot. After measuring the initial luminescence response to the normalization dose, a subset of aliquots was set aside for repetition, with the ratio of the secondary-to-initial luminescence responses defining a dose correction factor. Luminescence was measured using a Risø Model TL/OSL-DA-15 System containing light emitting diodes capable of either infrared (875 ± 30) or blue (470 ± 20) excitation. The resulting luminescence passes through a Hoya U-340 filters (>10% transmission >380 nm) prior to detection within the system's Thorn-EMI 9235 QA photomultiplier tube.

To eliminate any contributions to the luminescence signal from electrons residing within those traps that are thermally unstable over geologic time periods, two different heating treatments were employed: first, storage at 160°C for 1 h immediately following each laboratory irradiation (cf. Forman and Pierson, 2002); and second, measurement at an elevated temperature of 125°C during excitation (cf. Wintle and Murray, 2000). Because the natural luminescence

Table 1
Optical ages and associated data for sediments from the Mill Creek exposure, Indiana.

Field number	Laboratory number[a]	Equivalent dose (grays)	U (ppm)[b]	Th (ppm)[b]	K_2O (%)[b]	*a* value[c]	Dose rate (mGrays/yr)[d]	Optical age
MC0108-1	UIC2167IR	347.89 ± 2.88	1.7 ± 0.1	3.9 ± 0.1	1.67 ± 0.02	0.10 ± 0.01	2.29 ± 0.12	**149.2 ± 16.1**
MC0108-1	UIC2167BL	298.36 ± 5.69	1.7 ± 0.1	3.9 ± 0.1	1.67 ± 0.02	0.08 ± 0.01	2.22 ± 0.12	**134.6 ± 14.7**
MC0108-1	UIC2167Qz	279.01 ± 8.63	1.7 ± 0.1	3.9 ± 0.1	1.67 ± 0.02	0.07 ± 0.01	2.21 ± 0.12	**126.4 ± 13.9**
MC0108-2	UIC2168IR	464.07 ± 1.78	2.6 ± 0.1	7.0 ± 0.1	2.52 ± 0.03	0.07 ± 0.01	3.37 ± 0.17	**136.2 ± 14.5**
MC0108-2	UIC2168BL	436.46 ± 9.24	2.6 ± 0.1	7.0 ± 0.1	2.52 ± 0.03	0.06 ± 0.01	3.34 ± 0.17	**130.7 ± 14.1**
MC0108-2	UIC2168Qz	445.63 ± 3.83	2.6 ± 0.1	7.0 ± 0.1	2.52 ± 0.03	0.08 ± 0.01	3.47 ± 0.17	**128.6 ± 13.8**
MC0108-3	UIC2169IR	473.78 ± 9.20	3.0 ± 0.1	8.6 ± 0.1	2.96 ± 0.03	0.09 ± 0.01	4.14 ± 0.20	**114.5 ± 12.4**
MC0108-3	UIC2169BL	455.46 ± 2.79	3.0 ± 0.1	8.6 ± 0.1	2.96 ± 0.03	0.10 ± 0.01	4.22 ± 0.21	**107.9 ± 11.6**
MC0108-4	UIC2170IR	564.37 ± 6.17	3.4 ± 0.1	8.2 ± 0.1	2.94 ± 0.03	0.08 ± 0.01	4.12 ± 0.20	**137.1 ± 14.8**
MC0108-4	UIC2170BL	570.91 ± 6.87	3.4 ± 0.1	8.2 ± 0.1	2.94 ± 0.03	0.08 ± 0.01	4.17 ± 0.20	**137.0 ± 14.6**
MC930-1	UIC2421IR	341.35 ± 6.25	2.2 ± 0.1	4.6 ± 0.1	1.74 ± 0.02	0.09 ± 0.01	2.57 ± 0.13	**132.9 ± 14.3**
MC930-1	UIC2421BL	313.30 ± 1.52	2.2 ± 0.1	4.6 ± 0.1	1.74 ± 0.02	0.08 ± 0.01	2.48 ± 0.13	**126.2 ± 13.4**
MC930-1	UIC2421Qz	331.90 ± 3.47	2.2 ± 0.1	4.6 ± 0.1	1.74 ± 0.02	0.09 ± 0.01	2.54 ± 0.13	**130.4 ± 14.0**
MC930-2	UIC2420IR	374.95 ± 9.02	1.8 ± 0.1	4.3 ± 0.1	1.66 ± 0.02	0.09 ± 0.01	2.33 ± 0.12	**160.4 ± 17.5**
MC930-2	UIC2420BL	391.73 ± 3.11	1.8 ± 0.1	4.3 ± 0.1	1.66 ± 0.02	0.08 ± 0.01	2.31 ± 0.12	**169.8 ± 18.2**
MC930-2	UIC2420Qz	376.85 ± 2.85	1.8 ± 0.1	4.3 ± 0.1	1.66 ± 0.02	0.09 ± 0.01	2.33 ± 0.12	**160.2 ± 17.2**
							Unweighted mean and error	**136.4 ± 5.4**
							Standard deviation	**21.7**

All errors are at one sigma. Analyses by the Luminescence Dating Research Laboratory, University of Illinois at Chicago.

[a] Equivalent dose determined by the multiple aliquot regenerative dose technique (Jain et al. 2003) on the fine-grained (4–11 μm) polymineral extract with initial infrared (IR; 875 ± 30 nm) excitation, followed by blue light (BL; 470 ± 20 nm) excitation. Equivalent dose was also determined on fine-grained (4–11 μm) quartz separate under blue light excitation (Qz).

[b] U, Th and K_20 assayed by ICP-MS at Activation Laboratories, Ontario, Canada.

[c] Measured alpha efficiency factor (*a* value) as defined by Aitken and Bowman (1975).

[d] Dose rate included a cosmic ray dose rate component of 0.09 ± 0.01 grays/ka from calculations of Prescott and Hutton (1994) and an assumed burial moisture content of 30 ± 10%.

https://doi.org/10.1016/j.yqres.2009.10.008 Published online by Cambridge University Press

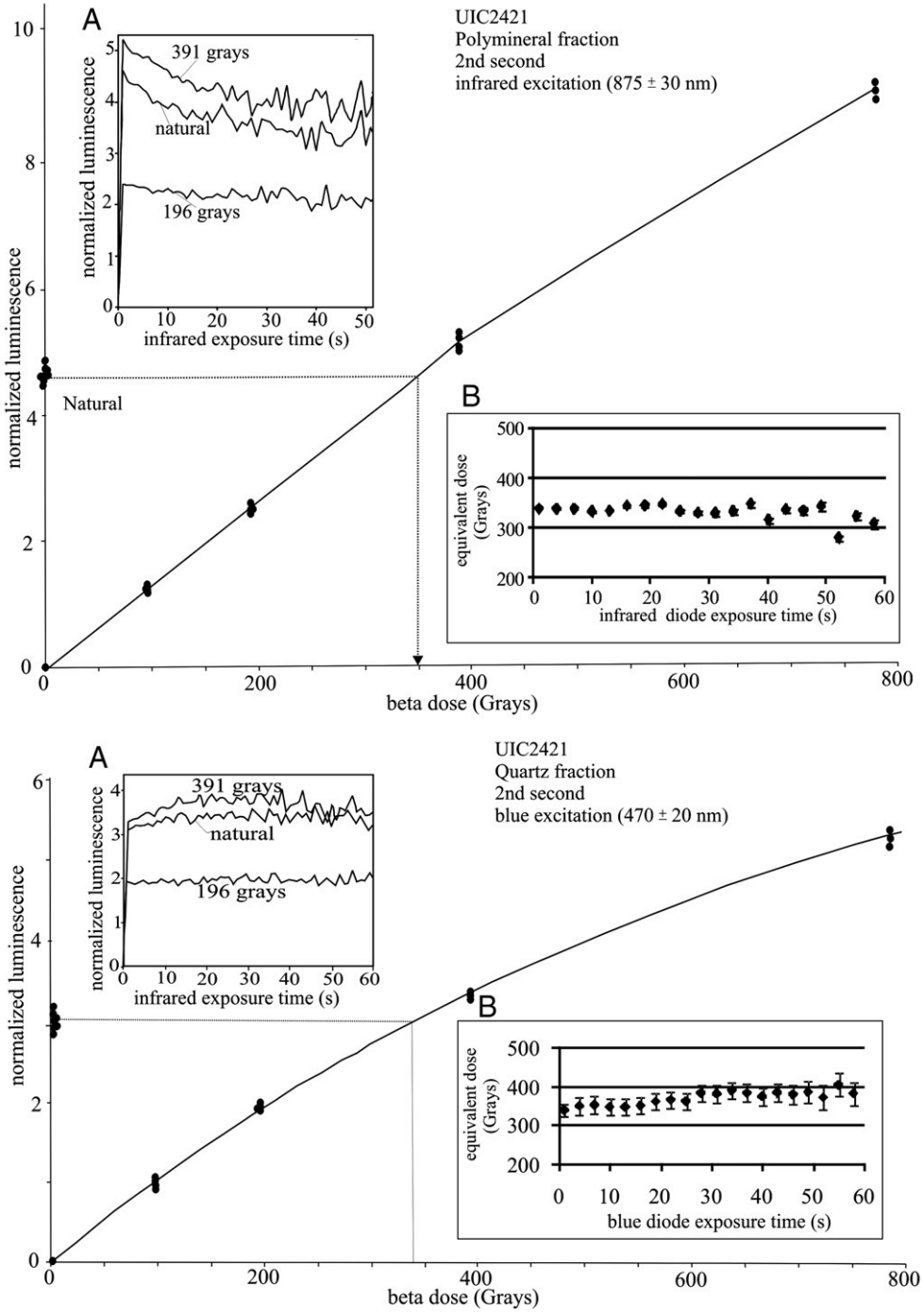

Figure 3. Regenerative dose response curve for sample UIC2421 from a finely laminated silt. Upper figure is for the fine-grained (4–11 μm) polymineral extract, lower for corresponding quartz extract. Inset figures (A) show natural luminescence normalized shine-down curves and associated regenerative dose response. Inset figures (B) shows equivalent dose for multiple light exposure times (plateau plot), including after 2 s, which is depicted in the main plot.

signal does not include any contributions from electrons residing within traps that are thermally unstable over geologic time periods, the first heating treatment is not required prior to its measurement. The temperature and duration of the first heating treatment following the subsequent normalization dose was selected from a range of temperatures (140–200°C) to mimic the charge distribution exhibited by the natural luminescence signal. Success was indicated by zero or low slope (<0.1) between the luminescence for initial and secondary dose, evaluated at 1-s intervals, and by a uniform equivalent dose value across the shine-down curve, also indicative of full solar resetting (Singarayer and Bailey, 2003). A sequential regenerative dose of >800 grays was applied to each sample that exceeded the corresponding natural luminescence and this dose response was unsaturated (Fig. 3). Equivalent dose was calculated for at least the first 20 s of excitation, dependent on background counts, as a weighted mean (Table 1).

We used laboratory procedures that access the light-sensitive luminescence components, particularly for quartz components. The most photosensitive traps for quartz are reset within 10 seconds of high-intensity (25 mW/cm^2) blue light (470 ± 20 nm) exposure (Agersnap-Larsen et al., 2000). These same traps are linked to the 325°C thermal luminescence peak, suggesting that its parent traps are

https://doi.org/10.1016/j.yqres.2009.10.008 Published online by Cambridge University Press

thermally stable over geologic timescales (lifetime $>3\times10^7$ yr at 20°C) (Wintle and Murray, 2000; Bulur et al., 2000) and are thus suitable targets for luminescence dating studies. This dating study used the blue light-emitting diode injection current that was limited to 10% of maximum, minimizing the photo-stimulation intensity and spreading the contributions from the various photosensitive traps over a much longer time period (20 s), increasing component resolution. The resulting distributions of the natural luminescence response with increasing photo-stimulation time for the Mill Creek sediments suggested full solar resetting, with a preheat treatment of 160°C for 1 h, yielding a luminescence distribution most similar to the natural emissions.

The MAR procedure determined two equivalent doses for each sample initially under infrared (IR) stimulation and then followed by blue stimulation (post IR-blue), similar to the so-called double, single aliquot regeneration protocols (Banerjee, 2001; Roberts et al., 2001). Infrared stimulation of polymineral fine-grained fraction of loess from midcontinent USA has yielded concordant ages with radiocarbon control and older ages that are consistent with stratigraphic control and other proxies (Forman and Pierson, 2002). The post-IR blue emissions may provide a more robust chronologic metric because initial infrared stimulation may reduce the feldspar luminescence signal, which is implicated in anomalous fading and age underestimates, whereas the subsequent blue excitation is believed to resolve the time-stable quartz luminescence (cf. Banerjee, 2001). However, a recent study has questioned the efficacy of post-infrared blue stimulation on isolating the quartz emissions, because of the dominance of the feldspar signal, which may show instability and lead to age underestimates (Roberts, 2007).

To evaluate the consistency of ages by infrared and post-IR blue stimulation, the corresponding quartz separate for four samples was analyzed under blue excitation. In turn, tests for anomalous fading on the IR, post-IR blue and blue-quartz emission over 30 days yielded no diminution in signal. It is important to note that ages by these three separate analytical approaches, IR, post IR-blue, and blue excitation of quartz separates overlap at one standard deviation, providing a consistent chronology.

To render an optical age the environmental dose rate is needed, which is an estimate of sediment exposure to ionizing radiation from the decay of the U and Th series and ^{40}K and cosmic sources during the burial period (Table 1). The U and Th content of sediment assuming secular equilibrium in the decay series and ^{40}K were determined by inductively coupled plasma-mass spectrometry analysed by Activation Laboratory LTD, Ontario, Canada. A small cosmic ray component of 0.09 ± 0.01 mGy/yr, for the indicated depth of sediment, was included in the estimated dose rate (Prescott and Hutton, 1994). Moisture content (by weight) for the dated sediments is 30 ± 10 % because the Mill Creek section exposes a perched water table on top of the diamicton. Water was observed emanating from the section throughout the year and served to lubricate active slumping, which enhanced exposure. In turn this site was also probably flooded by subsequent proglacial lakes during MIS 2 and 3 (Wood et al., 2007). The broad error (±10%) at two sigma spans the potential range of moisture contents during the burial period.

Sedimentologic context

The Mill Creek section is a cut bank exposure revealing more than 15 m of glacial and glaciolacustrine sediments (Figs. 4 and 5A). The basal unit (1) is >6 m thick and is a dense, stiff, and matrix-supported diamicton. This diamicton can be traced for several hundred meters along the stream bank. The matrix of the diamicton is a loam to a sandy loam and is carbonate-poor. Occasional to infrequent lenses of well-sorted and stratified coarse sand are present. Clasts 2 mm to 2 cm in diameter are common, and clasts >2 cm are rare, constituting on average of <5% by volume of the unit. Localized clast concentrations reach 10% to 15% by volume of the unit, and some large clasts have pebbles concentrated to one side (a stoss–lee configuration). Larger clasts are often bullet-shaped and display striations. Lithology of the >2 cm clasts is dominated by limestone, with minor amounts of fine-grained mafics, diorite, granite, quartzite, limonite, chert and sandstone. Orientation of clasts (30 clasts, 8–15 cm long axis) was plotted on a Schmidt equal-area net (Fig. 4) and contoured at a 2-sigma interval (cf. Lawson, 1979). The dispersion of the data is interpreted to cluster around a single mean axis and infer a direction of local ice flow toward S 21°W with an S_1 value of 0.7267. The upper 3–5 cm of unit 1 is weakly stratified and a single woody fragment was recovered within the upper 3 cm, which yielded a radiocarbon age of >45 ^{14}C ka BP (A1036). The upper boundary of unit 1 has a clear wavy contact with relief of 0.5–1.0 m.

Unit 2 shows variable sedimentology with a mix of well- to poorly sorted sediments. The lower 10 cm of unit 2 contains subcentimeter to centimeter-scale bedded silty sands and sandy silts. Beds closely conform to the underlying basal contact with unit 1, and are commonly disrupted by pebbles, which pierce and deform subjacent beds. Above the well-bedded sediments is crudely stratified to massive sandy silt to silty sand with common small pebbles. Bedding planes within this weakly bedded portion of the unit are denoted by infrequent lenses of well-sorted medium to coarse sand with herringbone-type cross bedding. Clasts (>2 cm) are rare and occur parallel with the bedding planes within the unit. Optical ages (Table 1) of 149.2 ± 16.1 ka (UIC 2167IR), 134.6 ± 14.7 (UIC2167BL) and 126.4 ± 13.9 ka (UIC2167Qz) are derived from IR stimulation, post-IR blue excitation of the polymineral fraction and blue stimulation on the quartz fraction from clayey-silt horizontal laminated sediments from the lower 10 cm of unit 2. The contact with the overlying unit 3 is somewhat gradual, represented by a transition zone 5–10 cm thick from weakly stratified sediments to a purely massive unit with intraclasts.

Unit 3 is a matrix-supported diamicton with common pebbles and intraclasts. The matrix is a firm silty sand. Intraclasts are common, vary in size (up to 40 cm in length) and have been plastically deformed (Fig. 5B). Lithic clasts >2 cm are uncommon, and those present are confined to the upper 5 to 10 cm of the unit and within bedding planes. The contact with the overlying unit 4 is abrupt.

Unit 4 displays a variable sedimentology and contains cm-scale low-angle cross beds ranging from a sandy silt to a medium to coarse sand. Beds within the eastern portion of the unit are overturned and parallel to the bedding plane (Fig. 5C). Near vertical and intersecting faults are present and display normal displacement upwards of 1–2 cm (Fig. 5C). Common small (2–5 cm) clasts and intraclasts are found throughout the unit and often disrupt and puncture bedding. A 2- to 5-cm-thick discontinuous bed of sandy silt with abundant intraclasts marks the contact between units 4 and 5 on the eastern side of the exposure. The sand lens has a maximum thickness of 6 cm and has been deformed into cm-scale diapir structures extending downward into the subjacent sediments. Beds observed in the upper portion of the unit are truncated and form an abrupt contact with unit 5.

Unit 5 is dominated by thinly bedded, horizontally laminated silts, with <5% clasts. Clasts and intraclasts (2- to 5-cm diameter) pierce and deform beds, and are common in the lower 15 cm of the unit but are rare throughout the remainder of the unit. The lower portion of the unit contains at least two distinct beds that grade from a coarse or medium sand to a fine silt. Flame structures are found within this lowest portion of the unit, which disrupt the overlying beds (Fig. 5D). The middle portion of the unit contains approximately 50 cm of finely laminated silts, with a few bed partitions denoted by a coarse to medium sand that grades to silt (Fig. 5E). Particle-size analysis shows that the finely laminated sediments are composed of 80–90% silt; the remainder is fine to very fine sand. The upper portion of the unit is

https://doi.org/10.1016/j.yqres.2009.10.008 Published online by Cambridge University Press

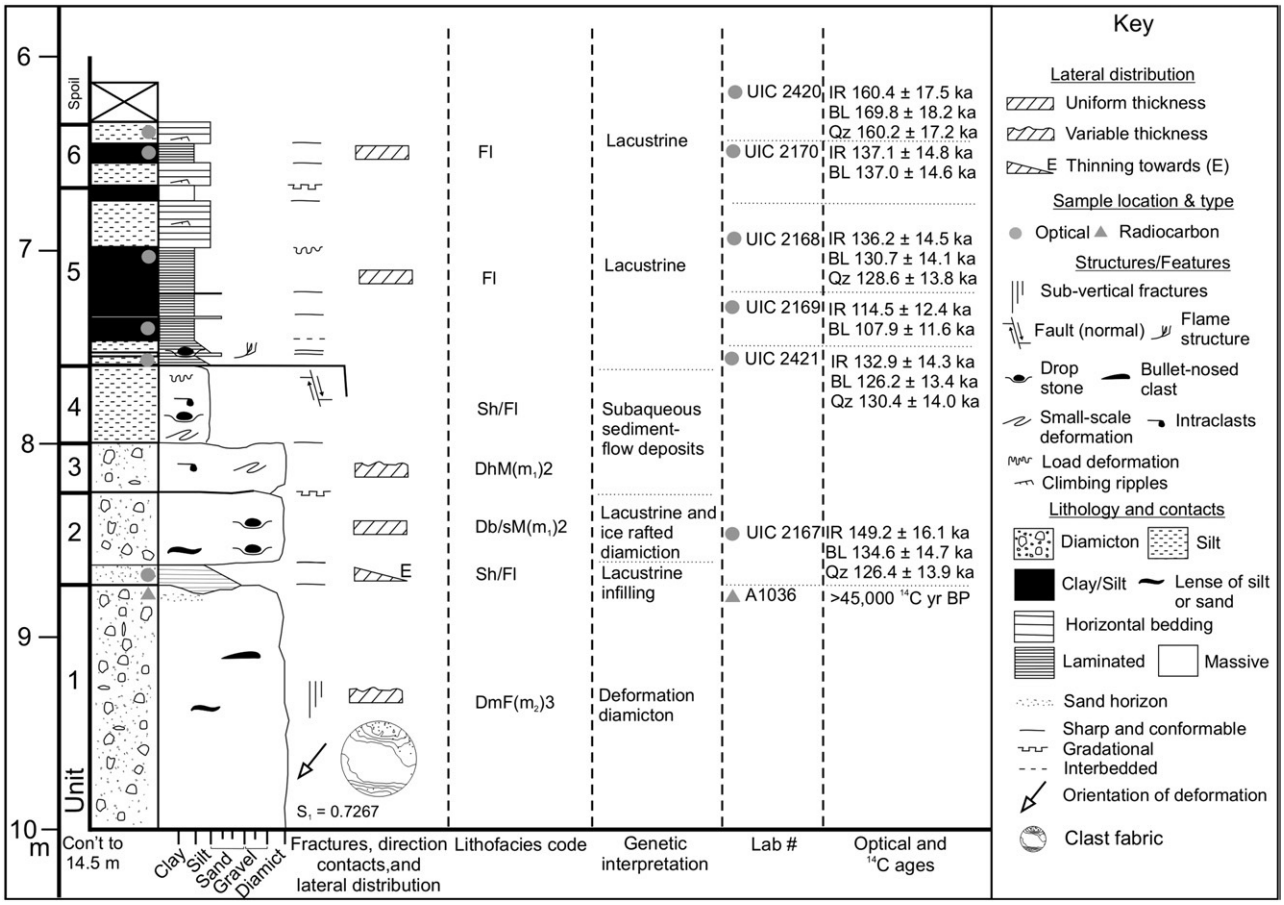

Figure 4. Stratigraphy and optical ages for lacustrine deposition of sediments associated with Glacial Lake Quincy at the Mill Creek section, Owen County, Indiana. Lithofacies codes adopted from Krüger and Kjaer (1999). Opposite unit 1 is associated fabric analysis of clasts.

composed of 15 cm of bedded sandy silt, capped by ~10 cm of dense massive silt. The sandy silt displays cm-scale, high-angle alternating climbing ripples. The massive silt capping the unit is cut by cm-scale fissures infilled by massive very fine sand to coarse silt. The contact with unit 6 is obscured by the fissures observed within the top of unit 5 but is gradational. Three sediments samples composed of finely laminated silts (UIC 2168, UIC 2169 and UIC 2421) yielded eight optical ages between ca. 136 and 108 ka (Table 1; Fig. 4).

Unit 6 contains mm- and cm-scale horizontal beds of silt and sandy silts. The lower 15 cm of unit 6 is characterized by cm-scale beds of sandy silt with high-angle climbing ripples. The middle of the unit contains approximately 10 cm of finely laminated silts and clayey silts. The upper 10 cm of the unit contains cm-scale beds of silt to sandy silt. High-angle climbing ripples are present but are confined to the lower 5 cm of this portion of the unit. Above unit 6 the remainder of the section is spoil. Two sediment samples (UIC 2170 and UIC 2420) were retrieved for optical dating (Table 1). A sample from the finely laminated silts yields optical ages of 137.1 ± 14.8 (UIC 2170IR) and 137.0 ± 14.6 (UIC 2170BL), derived from IR and post-IR blue excitation of the polymineral fraction. A sample from subcentimeter-scale silty beds yielded optical ages of 160.4 ± 17.5 ka (UIC 2420IR), 169.8 ± 18.2 (UIC2420BL) and 160.2 ± 17.2 ka (UIC2420Qz) and from IR stimulation, post-IR blue excitation of the polymineral fraction and blue stimulation on the quartz fraction, respectively.

Environmental interpretation

The diamicton of unit one has several characteristic features indicating genesis as a deformation diamicton of subglacial origin. In total the occurrence of clasts of various sizes and local (limestone) and exotic lithologies (grained mafics, diorite, granite, and quartzite) within a fine matrix and common striated and bullet-nosed clasts are indicative of subglacial transport (e.g., Krüger and Kjaer, 1999). The stoss–lee orientation and pebble clusters observed with some larger clasts is characteristic of pressure melting in a subglacial environment (Brodzikowski and van Loon, 1991, 246). The till fabric analysis yields a mean clast orientation to the SSW (Fig. 4) and the strong preferred orientation ($S_1 = 0.7267$) supports the interpretation for an origin from subglacial deformation (deformation till; cf. Lawson, 1979).

Sediments overlying the subglacial diamicton were deposited in a proglacial lacustrine environment. The upper few centimeters of the subglacial diamicton is weakly stratified, suggesting a wave-washed surface. Finely laminated sediments at the base of unit 2 reflect initial sediment deposition with formation of Glacial Lake Quincy, and it is apparently dominated by suspension-settling processes. The texture and structure of the sediments in units 2–6 indicate a transition from proximal to distal environments with respect to the retreating ice sheet margin (e.g., Harrison, 1975). The overall massive nature of units 2 and 3 are likely the result of debris flows from a diamicton source within or at the margin of the lake. The large clasts aligned parallel to bedding and found within units 2 and 3 are interpreted to be a lag from basal traction currents reworking fine-grained sediments. Pebbles observed disrupting the bedding of unit 2 are interpreted as ice-rafted debris, a diagnostic feature of ice-contact proglacial lakes (e.g., Ashley and Smith, 1985; Syverson, 1998). Clasts and intraclasts within the units originate as debris entrained within gravity-driven flows and as ice rafted detritus. Intraclasts entrained within debris flow are deformed, and one exceptional large intraclast (Fig. 5B) indicates an eastward direction for a mass movement. Gravity-driven sediment flows remain the dominant mechanism for

https://doi.org/10.1016/j.yqres.2009.10.008 Published online by Cambridge University Press

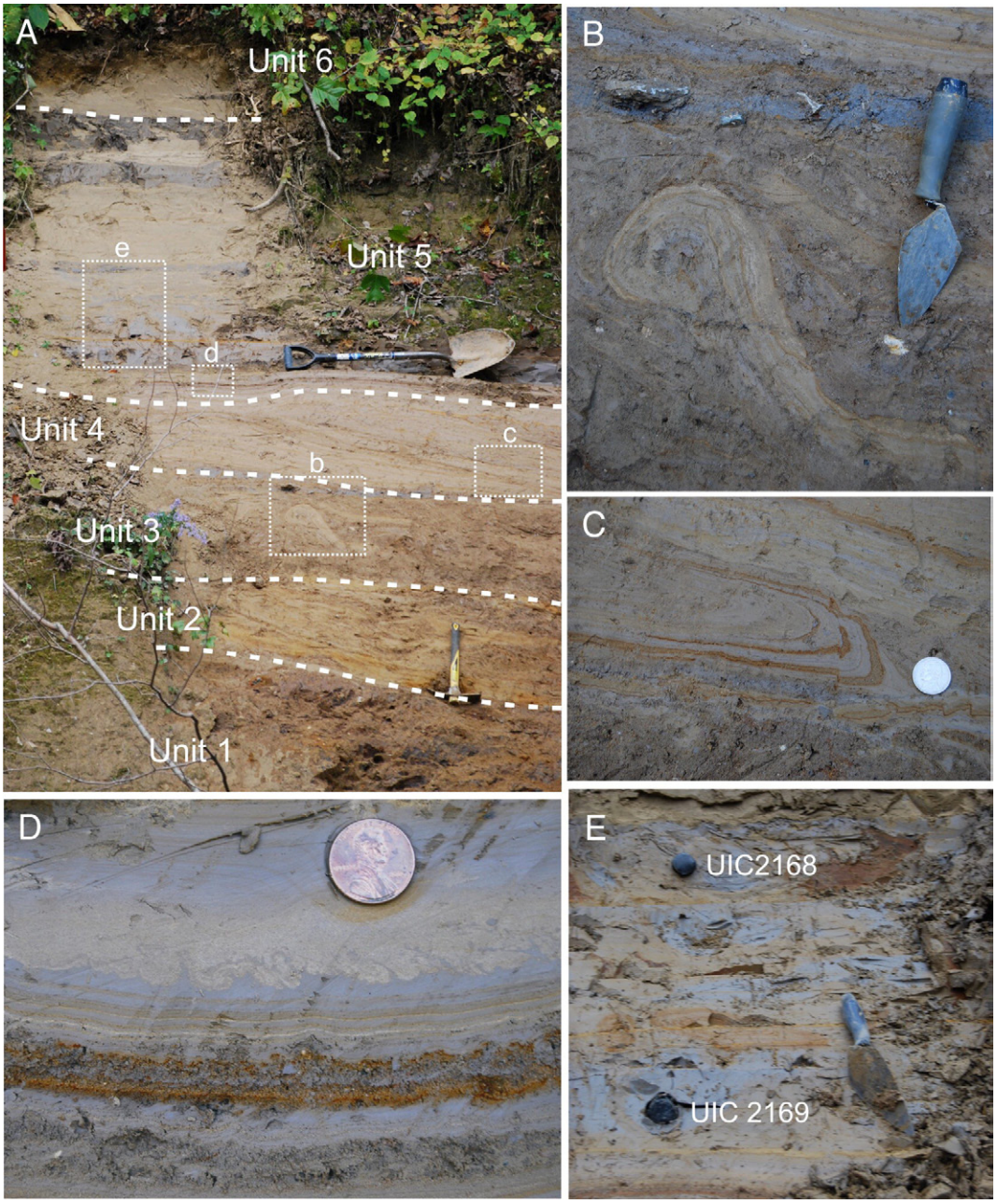

Figure 5. (A) Mill Creek section exposes a sequence of glacial lacustrine sediments representing ice proximal and ice distal environments over a subglacial diamicton. Shovel = 1 m. (B) Lacustrine diamicton resulting from melt-out sediments and ice rafted debris incorporated into mass debris flows. (C) Gravity-driven debris flow with overturn beds of fine-grained material within unit 4. Coin = 2.1 cm. (D) Flame structures from post-depositional dewatering of sediments within the lowest portion of unit 5. Coin = 1.9 cm. (E) Finely laminated silts found in unit 5 are targeted for optical dating.

deposition within unit 4. This unit contains thinly bedded sediments within obviously overturned layers and flow noses. Subsequent rapid sediment accumulation deposition above the contact between units 4 and 5 is indicated by the fractures and diapirs observed at the top of unit 4, consistent with waterlain sediment that have been subjected to compression driven dewatering (e.g., Ashley and Smith, 1985; Donnelly and Harris, 1989).

Rhythmically bedded fines composing units 5 and 6 are representative of proglacial bottom sets associated with suspension-settling environments distal from sediment sources (Donnelly and Harris, 1989; Brodzikowski and van Loon, 1991, 333). Bedding within units 5 and 6 is predominantly rhythmites, with couplets of silty and sandy beds and formed from changes in deposition rates, associated with suspension settling. The small-scale flame structures and the thick gradational beds indicate rapid deposition for the lower portion of section 5. The alteration between mm-scale horizontal silt beds and the cm-scale sandy silt beds are related to changes in sediment delivery at the glacial margin or oscillations in lake level as outlets open and close along Devore Ridge. The climbing ripples in the sandy silt beds reflect basal traction currents from material slumping either at the lake margin or at the lake-ice margin contact (Harrison, 1975; Donnelly and Harris, 1989). The alternating direction of the cross bedding indicates basal traction currents are from different directions within the lake.

Optical ages for Glacial Lake Quincy

The lithologic sequence at the Mill Creek section reflects retreat of an ice sheet lobe into a proglacial lacustrine environment. Sediments for optical dating were confined to the lowest depositional energy

https://doi.org/10.1016/j.yqres.2009.10.008 Published online by Cambridge University Press

facies, reflecting primary suspension settling with lateral transport through Glacial Lake Quincy. We contend that the high sensitivity of the dated luminescence components to solar resetting and uniformity of ages by feldspar and quartz components attests to uniform and low solar resetting and thus, optical ages date the time since deglaciation. Internal dating metrics including luminescence that mimics natural charge distribution and consistent equivalent dose plateau (Fig. 3) are consistent with the assumption of full solar resetting. Of particular note are the four ages on the fine-grained quartz fraction which overlap (at one sigma) with corresponding ages for the polymineral fraction. The quartz luminescence signal measured is particularly photosensitive, reset in full sunlight in seconds (Agersnap-Larsen et al., 2000) and is probably the most faithful geochronometer. However, it remains a possibility that the sediments were not completely solar reset prior to deposition and thus yielded age overestimates, but most likely within the two sigma age error (cf. Wintle, 1997).

The sixteen optical ages from proglacial lake bottom-set sediments, assuming that they are finite estimates, span from ca. 170 to 108 ka and yield a mean and average error of 136.4 ± 5.4 ka, with a standard deviation of 21.7 ka (Table 1). This age constraint place deglaciation from this Illinoian limit and formation of Glacial Lake Quincy late in MIS 6 near the transition to MIS 5, consistent with the classic Illinoian age assignment. Glacial Lake Quincy formed within approximately 15 km of the maximum Illinoian limit, early during deglaciation and is generally coincident with the rise in global sea level between MIS 6 and 5 (Fig. 6).

Glacial geologic associations

The sequence of sediments exposed along Mill Creek support the interpretation that Glacial Lake Quincy formed between an active glacier margin and Devore Ridge. The diamicton is inferred to be the result of a glacier advance prior to ca. 136 ka. This advance is associated with Illinoian diamictons and other lake sediments south of Devore Ridge and elsewhere within the Mill Creek Valley (e.g., Gray, 1988; Autio, 1990; Jacobs, 1994; Hall and Anderson, 2001). These glacial diamictons are correlated regionally by the stratigraphic relation with pronounced pedogenesis (Bt horizon) inferred to be the Sangamon Geosol (Willman and Frye, 1970; Jacobs, 1994; Hall and Anderson, 2000). Lake sediments and loess occur subjacent to two diamictons in the western end of Mill Creek Valley at the Cagles Mill section (Wayne, 1963; Hall and Anderson, 2000, 2001). The upper diamicton is inferred to be part of the Butlerville Till Member and the lower diamicton the Cloverdale Till Member of the Jessup Formation, both constituting the upper deposits of the Illinoian surface in southern Indiana (Wayne, 1963). The Sangamon Geosol is inferred to have developed within the upper glacial diamicton at the Cagles Mill section and a remnant of Yarmouth Geosol may be preserved in the lower diamicton (Hall and Anderson, 2001). The Sangamon Geosol has been also identified within a glacial diamicton observed in cores within the central part of the Mill Creek valley (Autio, 1990). The upper diamicton, hosting the Sangamon Geosol at the Cagle Mill site, may be correlative with glacial diamictons observed within the Flatwoods area (Fig. 1) with similar pedogenesis, approximately 20 km south of Mill Creek (Jacobs, 1994). Thus, the glacial diamicton observed in the Mill Creek section is inferred to be correlative to the upper glacial diamicton at the Cagles Mill section (Hall and Anderson, 2001) and in the Flatwood area (Jacobs, 1994). These diamictons are correlative with a surface diamicton of Illinoian drift, which is assigned to the Vandalia Till Member of the Glasford Formation of Illinois (Willman and Frye, 1970; Jacobs, 1994, p. 24), but questions remain of whether this member is correlative to the Jessup Formation in Indiana (Bleuer, 1991). This Vandalia Till Member is associated with a southwestern source possibly from a Saginaw-type lobe (Bleuer, 1991).

Central Indiana during the last glacial maximum (LGM) was a zone of confluence amongst the Erie, Huron and Saginaw lobes of the Laurentide ice sheet (Johnson, 1986; Fullerton, 1996). If the Illinoian ice sheet was lobate, similar to the LGM, then a Huron-Erie type lobe flowed across central Indiana into Illinois (Stiff and Hansel, 2004). A southwesterly ice flow direction is consistent also with the direction of striae observed locally on bedrock (Collett, 1876; Leverett, 1898) and the fabric analysis for the glacial diamicton (unit 1) from the Mill Creek exposure (Fig. 4). In turn, the upper glacial diamicton within the Flatwood area shows garnet to epidote ratios that reflect a potential Grenville provenance associated with glacier flow from an Erie-type lobe advancing toward the southwest (Jacobs, 1994). This lobe was probably characterized by low basal shear stress, moderate to high velocities, divergent flow and thicknesses of <400 m (Clark, 1992; Hooyer and Iverson, 2002) and may be particularly sensitive to mass balance changes near the terminus (cf. Lowell et al., 1999).

Conclusion

The formation of Glacial Lake Quincy provides insights to the deglaciation of one potential lobe of the Laurentide ice sheet in the Illinoian. This proglacial lake formed when the Illinoian ice sheet retreated ~15 km from its maximum limit, behind Devore Ridge, resulting in impoundment of meltwater. Lake level was controlled principally by outlets eroded into Devore Ridge, creating steep-walled canyons with waterfalls. The outlet elevations and location of lake sediments yield a lake area of at least 180 km^2 and >20 m deep. The section at Mill Creek documents retreat of the ice sheet into proglacial Lake Quincy with a succession from subglacial diamicton to ice-proximal to ice-distal glacial lacustrine sediments. Optical dating of the fine-grained polymineral and quartz fractions from the lowest energy depositional facies, lacustrine bottom sets, yielded a range of optical ages from ca. 170 to 108 ka, with a mean age of ca. 135 ka

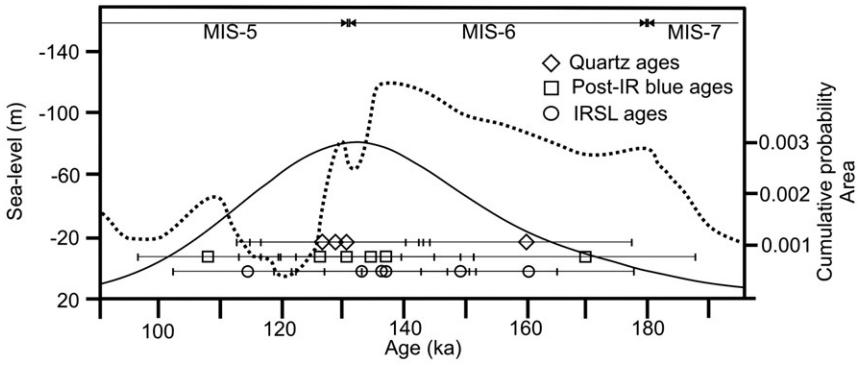

Figure 6. A comparison of optical ages from this study and global sea level curve (dashed line; Rohling et al., 1998). Optical ages range between 108 and 170 ka, with an average age of 136.4 ± 5.4 ka derived from an unweighted probability distribution (thin solid line). Error bars are 1 sigma.

https://doi.org/10.1016/j.yqres.2009.10.008 Published online by Cambridge University Press

(Fig. 6) age placing deglaciation at the transition from marine oxygen isotope stages 5 and 6, with the rise in global sea level (Rohling et al., 1998). The Illinoian deglacial optical ages of ca. 135 ka is consistent with optical ages on other Illinoian sediments including deposition of Loveland Loess at ca. 130–180 ka (Maat and Johnson, 1996; Rodbell et al., 1997; Markewich et al., 1998; Forman and Pierson, 2002) and proglacial fluvial sands deposited 190 to 160 ka (McKay and Berg, 2008). This association provides a direct chronologic constraint on the Illinoian till plain in southern Indiana, though additional studies are needed to resolve its potentially complex age structure.

Acknowledgments

This study was supported by graduate student research grants from the University of Illinois at Chicago, Geological Society of America and the Cave Research Foundation.

We are grateful to B. Raymer and D. Higgens for providing land access and field assistance of T. Chung and F. Schumann. The freeware utility StereoWin for Windows by R. Allmendinger was used for the fabric analysis. This paper benefited from the reviews of two anonymous reviewers and the editor, M. A. O'Neil.

References

Addington, A.R., 1926. Porter's Cave and recent drainage adjustments in its vicinity. Proceedings of the Indiana Academy of Science 36, 116–117.
Agersnap-Larsen, N., Bulur, E., McKeever, S.W.S., 2000. Use of LM-OSL for the detection of partial bleaching in quartz. Radiation Measurements 32 (5-6), 419–425.
Aitken, M.J., 1985. Thermoluminescence Dating. Academic Press, New York.
Aitken, M.J., Bowman, S.G.E., 1975. Thermoluminescent dating: assessment of alpha particle contribution. Archaeometry 17, 132–138.
Ashley, G.M., Smith, N.D., 1985. Proglacial Lacustrine Environment. In: Ashley, G.M., Shaw, J., Smith, N.D. (Eds.), Glacial Sedimentary Environments: Short Course 16. Society of Economic Paleontologists and Mineralogists, pp. 135–216.
Autio, R.J., 1990. Stratigraphy and geomorphology of the sediments of glacial lakes Quincy, Eminence, and Alaska, west-central Indiana. Masters Thesis, Indiana University, Bloomington, Indiana.
Banerjee, D., 2001. Supralinearity and sensitivity changes in optically stimulated luminescence of annealed quartz. Radiation Measurements 33, 47–57.
Berger, G.W., Mulhern, P.J., Huntley, D.H., 1980. Isolation of silt-sized quartz from sediments. Ancient TL 18, 7–11.
Bleuer, N.K., 1991. The Lafayette bedrock valley system of Indiana; concept, form and fill stratigraphy. In: Melhorn, W.N., Kempton, J.P. (Eds.), Geology and Hhydrology of the Teays-Mahomet Bedrock Valley System. Geological Society of America Special Paper 258, 51-78.
Brodzikowski, K., van Loon, A.J., 1991. Glacigenic Sediments. Elsevier Science Publishing Company, Inc., New York.
Brown, R.T., 1884. Geology of Morgan County. In: Collett, J. (Ed.), Indiana Department of Geology and Natural History; Thirteenth Annual Report, Indiana Department of Natural History, Indianapolis, 71-85.
Bulur, E., Bøtter-Jensen, L., Murray, A.S., 2000. Optically stimulated luminescence from quartz using linear modulation technique. Radiation Measurements 32 (5-6), 407–411.
Clark, P.U., 1992. Surface form of the Southern Laurentide ice sheet and its implications to ice sheet dynamics. Geological Society of America Bulletin 104, 595–605.
Collett, J., 1876. The Geology of Owen County. In: Cox, E.T., (Ed.), Indiana Department of Geology and Natural History, Seventh Annual Report, Geological Survey of Indiana, Indianapolis, pp. 301-360.
Curry, B.B., 1989. Absence of Altonian glaciation in Illinois. Quaternary Research 31, 1–13.
Curry, B.B., Pavich, M.J., 1996. Absence of glaciation in Illinois during marine isotope stages 3 through 5. Quaternary Research 46, 19–26.
Donnelly, R., Harris, C., 1989. Sedimentology and origin of deposits from a small ice-dammed lake, Leirbreen, Norway. Sedimentology 36, 581–600.
Flint, R.F., 1971. Glacial and Quaternary Geology. John Wiley and Sons, New York.
Follmer, L.R., 1983. Sangamon soil and Wisconsinan pedogenesis in the midwestern United States. In: Porter, S.C. (Ed.), Late-Quaternary Environments of the United States: The Pleistocene. University of Minnesota Press, Minneapolis, pp. 138–144.
Follmer, L.R., 1996. Loess studies in the central United States: evolution of concepts. Engineering Geology 45, 287–304.
Forman, S.L., Pierson, J., 2002. Late Pleistocene luminescence chronology of loess deposition in the Missouri and Mississippi river valleys, United States. Palaeogeography, Palaeoclimatology, Palaeoecology 186, 25–46.
Frye, J.C., 1968. Development of Pleistocene stratigraphy in Illinois. In: Bergstrom, R.E. (Ed.) ,The Quaternary of Illinois. University of Illinois and Illinois State Geological Survey, pp. 3-10.
Frye, J.C., Willman, H.B., Black, R.F., 1965. Outline of Glacial Geology of Illinois and Wisconsin. In: Wright, H.E., Frey, D.G. (Eds.), The Quaternary of the United States. Princeton University Press, Princeton, pp. 43–61.
Fullerton, D.S., 1996. Stratigraphy and correlation of glacial deposits from Indiana to New York and New Jersey. Quaternary Science Reviews 5, 23–37.
Godfrey-Smith, D.I., Huntley, D.J., Chen, W.H., 1988. Optical dating studies of quartz and feldspar sediment extracts. Quaternary Science Reviews 7, 373–380.
Gray, H.H., 1988. Relict Drainageways Associated with the Glacial Boundary in Southern Indiana. Department of Natural Resources - Geological Survey, Bloomington pp 9.
Grimley, D.A., 2000. Glacial and nonglacial sediment contributions to Wisconsin Episode loess in the central United States. Geological Society of America Bulletin 112 (10), 1475–1495.
Hall, R.D., Anderson, A.K., 2000. Comparative soil development of quaternary paleosols of the central United States. Palaeogeography Palaeoclimatology Palaeoecology 158, 109–145.
Hall, R.D., Anderson, A.K., 2001. Quaterary record at Cagles Mill, Putnam County, Indiana. Proceedings of the Indiana Academy of Science 110, 9–22.
Harrison, S.S., 1975. Turbidite Origin of Glaciolacustrine Sediments, Woodcock Lake, Pennsylvania. Journal of Sedimentary Petrology 45, 738–744.
Hooyer, T.S., Iverson, N.R., 2002. Flow mechanism of the Des Moines lobe of the Laurentide ice sheet. Journal of Glaciology 48, 575–586.
Jacobs, P.M., 1994. Stratigraphy, Landscape Evolution, and a Pleistocene Buried Soil lithosequence in the Flatwoods Region of Owen and Monroe Counties, Indiana. Ph. D. Thesis, University of Wisconsin-Madison.
Jain, M., Botter-Jensen, L., Singhvi, A.K., 2003. Dose evaluation using multiple-aliquot quartz OSL: test of methods and a new protocol for improved accuracy and precision. Radiation Measurements 37, 67–80.
Jennings, C.E., Aber, J.S., Balco, G., Barendregt, R., Bierman, P.R., Rovey, C.W., Thorleifson, L.H., Mason, J.A., 2007. Mid-quaternary in North America. In: Elias, S.A. (Ed.), Encyclopedia of Quaternary Sciences. Elsevier, Amsterdam, pp. 1044–1051.
Johnson, W.H., 1986. Stratigraphy and correlation of the glacial deposits of the Lake Michigan Lobe prior to 15 ka BP. In: Sibrava, V., Bowen, D.Q., Richmond, G.M. (Eds.), Quaternary Glaciations in the Northern Hemisphere. Pergamon Press, New York, pp. 17–22.
Joyce, E.J., Tjalsma, L.R.C., Prutzman, J.M., 1993. North American glacial meltwater history for the past 2.3 m.y.: oxygen isotope evidence from the Gulf of Mexico. Geology 21, 483–486.
Krüger, J., Kjaer, K.H., 1999. A data chart for field description and genetic interpretation of glacial diamicts and associated sediments — with examples from Greenland, Iceland, and Denmark. Boreas 28, 386–402.
Lawson, D.E., 1979. Sedimentological analysis of the western terminus region of the Matanuska Glaciaer, Alaska. US Army Cold Regions Research and Engineering Laboratory, Hanover, p. 122.
Leverett, F., 1898. The weathered zone (Yarmouth) between the Illinoian and Kansan till sheets. Journal of Geology 6, 238–243.
Lowell, T.V., Hayward, R.K., Denton, G.H., 1999. Role of Climate oscillations in determing ice-margin position: Hypothesis, examples and implications. In: Mickelson, D. M., Attig, J.W. (eds.), Special Paper 337: Glacial Processes Past and Present. Geological Society of America, Denver, pp193-203.
Maat, P.B., Johnson, W.C., 1996. Thermoluminescence and new C-14 age estimates for late Quaternary loesses in southwestern Nebraska. Geomorphology 17, 115–128.
Malott, C.A., 1922. The physiography of Indiana. In: Logan, W.N., Cumings, E.R., Malott, C.A., Visher, S.S., Tucker, W.M., Reeves, J.R (Eds.), Handbook of Indiana geology. Indiana Department of Conservation Publication, Indianapolis, pp. 210–211.
Malott, C.A., 1926. The Glacial Boundary in Indiana. The Proceedings of the Indiana Academy of Science 35, 93–107.
Markewich, H.W., Wysocki, D.A., Pavich, M.J., Rutledge, E.M., Millard, H.T., Rich, F.J., Maat, P.B., Rubin, M., McGeehin, J.P., 1998. Paleopedology plus TL, ^{10}Be, and ^{14}C dating as tools in stratigraphic and paleoclimatic investigations, Mississippi River Valley, U.S.A. Quaternary International 51-52 143–167.
McGrain, P., 1949. Geological features of the proposed Cagle's Mill flood control reservoir. The Proceedings of the Indiana Academy of Science 58, 163–172.
McKay, D.E., Berg, R.C., 2008. Optical ages spanning two glacial-interglacial cycles from deposits of the Ancient Mississippi River, north-central Illinois. Geological Society of America Abstracts and Programs 40 (5), 78.
Prescott, J.R., Hutton, J.T., 1994. Cosmic ray contributions to dose rates for luminescence and ESR dating: Large depths and long-term time variations. Radiation Measurements 23, 497–500.
Rendell, H.M., Webster, S.E., Sheffer, N.L., 1994. Underwater bleaching of signals form sediment grains: new experimental data. Quaternary Science Reviews 13, 433–435.
Richardson, C.A., 1994. Effects of bleaching on the sensitivity to dose of the infrared-stimulated luminescence of potassium-rich feldspars from Ynyslas, Wales. Radiation Measurements 23, 587–591.
Roberts, H.M., 2007. Assessing the effectiveness of the double-SAR protocol in isolating a luminescence signal dominated by quartz. Radiation Measurements 42, 1627–1636.
Roberts, H.M., Wintle, A.G., Maher, B.A., Hu, M.Y., 2001. Holocene sediment-accumulation rates in the western Loess Plateau, China, and a 2500-year record of agricultural activity, revealed by OSL dating. Holocene 11, 477–483.
Rohling, E.J., Fenton, M., Jorissen, F.J., Bertrand, P., Ganssen, G., Caulet, J.P., 1998. Magnitudes of sea-level lowstands of the past 500,000 years. Nature 394, 162–165.
Rodbell, D.T., Forman, S.L., Pierson, J., Lynn, W.C., 1997. Stratigraphy and chronology of Mississippi Valley loess in western Tennessee. Geological Society of America Bulletin 109, 1134–1148.
Ruhe, R.V., 1969. Quaternary Landscapes in Iowa. Iowa State University Press, Ames, Iowa.

https://doi.org/10.1016/j.yqres.2009.10.008 Published online by Cambridge University Press

Sanderson, D.C.W., Bishop, P., Stark, M., Alexander, S., Penny, D., 2007. Luminescence dating of canal sediments from Angkor Borei, Mekong Delta, southern Cambodia. Quaternary Geochronology 2, 322–329.
Singarayer, J.S., Bailey, R.M., 2003. Further investigations of the quartz optically stimulated luminescence components using linear modulation. Radiation Measurements 37, 451–458.
Stiff, B.J., Hansel, A.K., 2004. Quaternary Glaciations in Illinois. In: Ehlers, J., Gibbard, P.L. (Eds.), Developments in Quaternary Science: Quaternary Glaciations-Extent and Chronology: Part II. North America. Elsevier, Amsterdam, pp. 71–82.
Syverson, K.M., 1998. Sediment record of short-lived ice-contact lakes, Burroughs Glacier, Alaska. Boreas 27, 44–54.
Thornbury, W. D., 1936. Glacial geology of southern and south-central Indiana. Ph.D Dissertation, Indiana University, Bloomington, Indiana.
Thornbury, W.D., 1940. Glacial lakes quincy and eminence. Indiana Academy of Sciences Proceedings 49, 131–144.
Thornbury, W.D., 1950. Glacial Sluiceways and Lacustrine Plains of Southern Indiana. Indiana Department of Conservation – Division of Geology, Bloomington, p. 21.
Tripsanas, E.K., Bryant, W.R., Slowey, N.C., Bouma, A.H., Karageorgis, A.P., Berti, D., 2007. Sedimentological history of Bryant Canyon area, northwest Grulf of Mexico, during the last 135 kyr (Marine Isotope Stages 1–6): a proxy record of Mississippi River discharge. Palaeogeography Palaeoclimatology Palaeoecology 246 (1), 137–161.
Wang, H., Lundstrom, C.C., Zhang, Z., Grimley, D.A., Balsam, W.L., 2009. A mid-late quaternary loess-paleosol record in Simmons Farm in southern Illinois, USA. Quaternary Science Reviews 28, 93–106.
Wayne, W. J., 1963. "Pleistocene formation in Indiana." Indiana Department of Conservation Geological Survey, Bloomington, Indiana, 85pp.
Willman, H. B., Frye, J. C., 1970. Pleistocene Stratigraphy of Illinois. Illinois State Geological Survey, Champaign, pp 204.
Wintle, A.G., 1997. Luminescence dating: laboratory procedures and protocols. Radiation Measurements 27, 769–817.
Wintle, A.G., Murray, A.S., 2000. Quartz OSL: effects of thermal treatment and their relevance to laboratory dating procedures. Radiation Measurements 32, 387–400.
Wood, J.R., Forman, S.L., Everton, D.W., 2007. The extent and timing of a pre-late Wisconsinan ice margin in central Indiana; a new view from glacial-lacustrine sediments from Porter Cave (abstract). Journal of Cave and Karst Studies 69, 369.

https://doi.org/10.1016/j.yqres.2009.10.008 Published online by Cambridge University Press